Eur Biophys J (1991) 20:127–133

European Biophysics Journal

Single point mutations of the sodium channel drastically reduce the pore permeability without preventing its gating

M. Pusch[1,2], M. Noda[2]*, W. Stühmer[2], S. Numa[3], and F. Conti[1]

[1] Istituto di Cibernetica e Biofisica, CNR, Via Dodecaneso 33, I-16146 Genova, Italy
[2] Max-Planck-Institut für biophysikalische Chemie, Am Fassberg, W-3400 Göttingen, Federal Republic of Germany
[3] Departments of Medical Chemistry and Molecular Genetics, Kyoto University Faculty of Medicine, Kyoto, 606 Japan

Received March 21, 1991/Accepted in revised form June 17, 1991

Abstract. *1.* Two mutants of the sodium channel II have been expressed in *Xenopus* oocytes and have been investigated using the patch-clamp technique. In mutant E387Q the glutamic acid at position 387 has been replaced by glutamine, and in mutant D384N the aspartic acid at position 384 has been replaced by asparagine. *2.* Mutant E387Q, previously shown to be resistant to block by tetrodotoxin (Noda et al. 1989), has a single-channel conductance of 4 pS, that can be easily measured only using noise analysis. At variance with the wild-type, the open-channel current-voltage relationship of mutant E387Q is linear over a wide voltage range even under asymmetrical ionic conditions. *3.* Mutant D384N has a very low permeability for any of the following ions: Cl^-, Na^+, K^+, Li^+, Rb^+, Ca^{2+}, Mg^{2+}, NH_4^+, TMA^+, TEA^+. However, asymmetric charge movements similar to the gating currents of the Na^+-selective wild-type are still observed. *4.* These results suggest that residues E387 and D384 interact directly with the pathway of the ions permeating the open channel.

Key words: Sodium channel – Gating current – Noise analysis – Site-directed mutagenesis – Tetrodotoxin

Introduction

In studying voltage-gated Na^+ channels in nerve cells, the high affinity blocker tetrodotoxin (TTX) has been a valuable tool (Hille 1984). Binding of TTX to the Na^+ channel protein is thought to occur near the extracellular entrance of the channel pore. Recently, a TTX-insensitive mutant of Na^+ channel II was described (Noda et al. 1989). In this mutant, the negative glutamic acid (E) at position 387 is replaced by an uncharged glutamine (Q) (hence mutant "E387Q"). Position 387 is located towards the C-terminal end of the sequence connecting segments S5 and S6 in repeat I of Na^+ channel II (Noda et al. 1986a). This connecting sequence has also been shown to be involved in the binding of α-scorpion toxins that modify inactivation (Tejedor and Catterall 1988), and might even contain part of the pore lining structure (Guy and Conti 1990).

If residue E387 is involved in TTX binding and located near the extracellular entrance of the open pore, we expect that the mutation E387Q and mutations involving neighbouring amino acids may significantly alter permeability properties. Indeed, for mutant E387Q the ratio of the gating currents to the ionic currents is larger than in the wild-type channel. From this observation, Noda et al. (1989) suggested that the conductance of this mutant is much lower than that of the wild-type. This makes it very difficult to record directly single-channel currents. In this paper we report more detailed measurements of the conductance properties of mutant E387Q using "tail" currents and non-stationary noise analysis.

If a mutant channel has a very low single-channel conductance, γ, as a consequence of a drastic change of an essential part of the ion conduction pathway, its expression in *Xenopus* oocytes cannot be easily detected electrophysiologically. However, if the gating mechanism is preserved, charge movements associated with the voltage-dependent conformational changes ("gating currents", Armstrong and Bezanilla 1973), should still be measurable as in the case of the wild-type channel (Conti and Stühmer 1989). We report here the case of mutant D384N in which the aspartic acid D384, three residues apart from position 387, has been replaced by an asparagine. Large gating currents reveal a high yield of exogenous expression of this channel protein in cell-attached and inside-out patches of frog oocytes, although

Abbreviations: TTX, tetrodotoxin; Na^+, sodium; K^+, potassium; NFR, normal frog Ringer; HEPES, N-2-hydroxylethyl piperazine-N'-2-ethanesulfonic acid; EGTA, ethyleneglycol-bis(β-amino-ethyl ether) N,N,N',N'-tetra acetic acid; TEA, tetraethylammonium; TMA, tetramethylammonium; I_g, gating current; γ, single-channel conductance

* *Present address:* Max-Planck-Institut für Entwicklungsbiologie, W-7400 Tübingen, Federal Republic of Germany
Offprint requests to: M. Pusch

the conductance of the channel is so low that macroscopic ionic currents are barely detectable.

A short preliminary report of these results has been presented (Pusch et al. 1991).

Methods

RNA preparation

The aspartic acid residue 384 of rat sodium channel II (Noda et al. 1986a) was mutated to asparagine (D384N) using the synthetic oligonucleotide 5′–ATA AAG GTT TTC CCA GAA GTT TTG AGT CAT GAG–3′ according to the procedure described by Noda et al. (1989). mRNAs specific for the mutant sodium channels D384N (plasmid pRIICM-2) and E387Q (plasmid pRIICM-1) were synthesized in vitro using SalI-cleaved plasmids as templates (Noda et al. 1986b, 1989).

Xenopus laevis oocytes were isolated and injected with ≈20 ng of mRNA and incubated at 18 °C as described by Stühmer et al. (1987). After two days of incubation the follicular layer was removed. After at least two more days of incubation the vitelline membrane was removed twenty minutes prior to the experiments (Methfessel et al. 1986) and the oocytes were transferred to the recording chamber.

Solutions

Normal frog Ringer (NFR) was the most frequently used pipette filling solution (except where indicated) and had the following composition (in m*M*): 115 NaCl, 10 NaOH-HEPES, 2.5 KCl, 1.8 $CaCl_2$, pH 7.2. Other solutions are listed in the figure legends. Experiments were performed at 15 °C.

Current recording

Conventional patch-clamp techniques (Hamill et al. 1981) were used for current recording. Macroscopic currents were recorded from large cell-attached or inside-out patches using pipettes pulled from aluminosilicate glass (Hilgenberg). The pipettes were constructed with a fairly wide tip opening and had resistances between 0.5 and 1.5 MΩ in Ringer. Current recording and stimulation were controlled by DEC PDP-11/73 minicomputer. Currents were filtered at 10 kHz with an eight-pole-Bessel filter (npi electronic) and digitized at 50 or 100 kHz. Ionic currents and in some cases also gating currents were corrected on-line for linear leakage and capacitive currents using a P/4-method (Bezanilla and Armstrong 1977) setting the control voltage of the P/4 pulses to −140 mV.

In order to optimize the signal-to-noise ratio a different pulse protocol was usually applied in gating current measurements. A typical pulse protocol consisted of alternating series of test and "leak" pulses. Leak pulses to either −100 or −160 mV were applied from a control voltage of −130 mV on the assumption that in this voltage range a negligible gating current flows. These pulses were used off-line for linear leakage and capacitance correction as described by Conti et al. (1984) and Conti and Stühmer (1989).

A similar pulse protocol was used for the collection of large ensembles of test and control sweeps used for the non-stationary noise analysis.

Non-stationary noise analysis

Non-stationary noise analysis of sodium-channel currents allows the determination of the single-channel current from macroscopic current fluctuations (Sigworth 1977) and is particularly useful when single-channel current measurements are difficult to perform. The basic assumptions underlying this method are that the current fluctuations arise solely from conductance fluctuations of a homogeneous population of independent channels having only one level of non-zero conductance.

For the experiments shown in Fig. 2, at least 100 leak-subtracted pulses to a fixed voltage were used to determine the single-channel current, *i*. Leak subtraction and noise-analysis were done according to the procedure described by Conti et al. (1980) (see also Heinemann and Conti 1991).

Results

Conductance properties of mutant E387Q

We studied the conductance properties of the TTX-insensitive Na^+ channel mutant E387Q (Noda et al. 1989) in more detail because the TTX binding site has been suggested to be implicated in the conduction process of the Na^+ channel (Hille 1975). Conductance properties are best studied using single-channel measurements. However, for channels, like E387Q, that open briefly and have low-conductance, single-channel measurements are difficult to perform. Therefore, we measured instantaneous current-voltage relationships from tail currents and, in addition, we performed non-stationary noise analysis. Both types of measurement were done on inside-out patches, in order to control the Na^+ concentration on both sides of the membrane, and to avoid blockage by internal Mg^{2+} which is known to produce inward rectification in cell-attached patches (Pusch et al. 1989).

Figure 1 shows instantaneous current-voltage relationships (I-V's) derived from tail-current traces (shown as insets) in two different patches with different internal Na^+ concentration, $[Na]_i$, and NFR as extracellular solution. Squares are data obtained with $[Na]_i = 30$ m*M*; circles are data for $[Na]_o \approx [Na]_i = 100$ m*M*, scaled to yield the same slope conductance of the asymmetric conditions. The dotted line shows, for comparison, the I-V of the wild-type for the same asymmetric conditions, scaled to yield the same asymptotic slope conductance at high voltages. For the asymmetric conditions the reversal potential, E_r, is close to the expected Nernst equilibrium

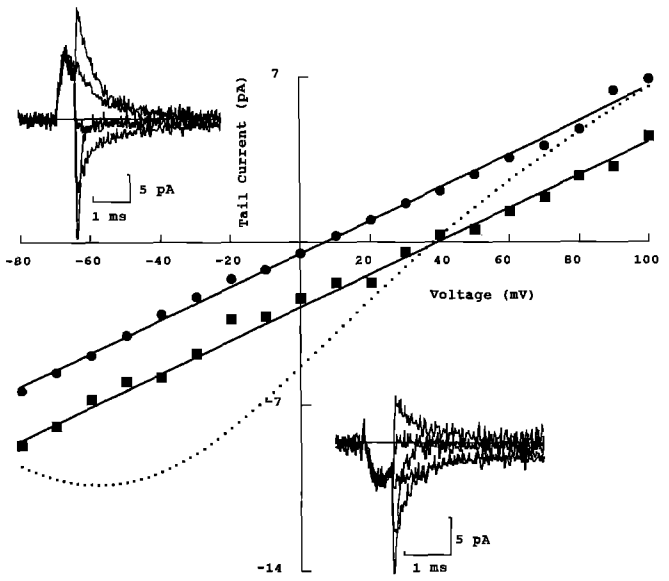

Fig. 1. Instantaneous current-voltage relationships of mutant E387Q. Tail current traces (shown in the insets) were measured on two different inside-out patches with NFR in the pipette from an oocyte injected with mRNA specific for mutant E387Q. The tail currents were used to construct instantaneous I–V's as described in Pusch et al. (1989). The bath (internal) solution contained (in m*M*) 30 m*M* NaCl, 90 m*M* KCl, 10 m*M* HEPES-KOH, 10 m*M* EGTA-KOH, pH 7.2 for the filled squares ("asymmetric") and 100 m*M* NaCl, 10 m*M* HEPES-KOH, 10 m*M* EGTA-KOH, pH 7.2 for the filled circles ("symmetric"). The solid lines are linear regression lines with a correlation coefficient of $r=0.99$ in both cases. The "symmetric" I–V has been scaled such that the slopes of the lines coincide. The dotted line is the wild-type instantaneous I–V as reported by Pusch et al. (1989) for the same "asymmetric" conditions, scaled to yield the same asymptotic slope conductance at large voltages. The insets show sample records with "tail" voltages of −80, −40, 0, 40 and 80 mV. Conditioning voltages were 10 mV (filled squares) or 30 mV (filled circles). Linear leakage and capacitive currents were subtracted by a P/4 method

potential for Na^+, E_{Na}, ($E_r \approx 35$ mV, $E_{Na}=36$ mV) showing that the channel is highly selective for Na^+ over K^+ like the wild-type (Pusch 1990a). However, the I-V's are linear over a wide voltage range (correlation coefficient $r=0.99$). This behavior is different from that of the wild-type I-V which shows inward rectification (Pusch et al. 1989; Pusch 1990a) and an upward deflection at low voltages (<-30 mV) due to block by external Ca^{2+} (Pusch 1990b).

On the basis of the comparison of the sizes of gating and ionic currents Noda et al. (1989) estimated that mutant E387Q has approximately a 4-fold lower conductance than the wild-type channel. From non-stationary channel-noise analysis (Sigworth 1977; Heinemann and Conti 1991) we have obtained for mutant E387Q estimates of the single-channel current, i(V), at several voltages V. Figure 2B shows typical mean current and variance traces for two test voltages. For both voltages a relatively large gating current at the initial part of the current trace is visible, which indicates that the conductance of the channel is rather low, as noticed by Noda et al. (1989). In Fig. 2C the corresponding variance-current plots are illustrated. The solid lines in Fig. 2B represent fits of a parabolic function as described by Heinemann and Conti (1991) yielding i(V). An i-V plot for one patch is shown in Fig. 2A. It can be seen that the current-voltage relationship is linear in the voltage range investigated (−60 to 10 mV) in agreement with the macroscopic instantaneous I-V measurements. From its slope a single-channel conductance of 4 pS can be estimated. Data of this type from five different inside-out patches yielded a mean conductance of 4.1 ± 0.3 pS. This value is $\approx$5-fold lower than the slope conductance reported by Stühmer et al. (1987) for the wild-type channel as measured in cell-attached patches in the voltage range of −60 to 0 mV.

Qualitative features of mutant D384N

Four days after injection of mRNA specific for the mutant Na^+ channel D384N, nonlinear current responses to step-voltage stimulations could be observed as displayed in Fig. 3. Figure 3A shows three P/4 corrected records, obtained from a cell-attached patch with NFR in the pipette by pulsing the membrane voltage from −100 mV to the indicated values. A sharply rising and rapidly decaying positive current is observed after the onset of each voltage step. At the end of the pulse, a similar charge movement occurs in the opposite direction. During the pulse to 0 mV, a smaller and slower inward current component can also be seen. We tentatively attribute this current to sodium ions (see later) and denote it I_{Na}. The characteristics of the major (fast) component of these responses are similar to those of sodium gating currents, I_g, observed in natural excitable cells (Almers 1978), and in oocytes injected with mRNA specific for the wild-type sodium channel II (Conti and Stühmer 1989).

Such currents are absent in oocytes not injected with exogenous mRNA. Therefore we must conclude that mutant D384N is expressed in the membrane at a high enough density to produce readily detectable gating currents, although the resulting channel protein is unable to produce the large increase of membrane permeability to Na^+ that characterizes the functioning of normal Na^+ channels.

By comparison with the properties of wild-type channels, and assuming that the gating charge per channel is the same (see later), the relative size of the I_g near the reversal potential and the maximum peak inward I_{Na} indicates that the conductance of mutant D384N is in the range of 10–40 fS, which is 3 orders of magnitude lower than that of the wild-type.

The small inward current that is most apparent in the 0 mV record of Fig. 3A is not blocked by 1 μ*M* TTX in the pipette (Fig. 3B). In this respect, mutant D384N is similar to mutant E387Q (Noda et al. 1989). However, owing to the small size of the ionic currents, it is difficult to estimate the TTX sensitivity quantitatively.

For the same reason we could only obtain qualitative information on the ionic selectivity of the pathway of these currents. It appears to be selective for Na^+ versus Cl^- because negative currents are observed at 0 mV (Figs. 3A, 3B), above the negative equilibrium potential for Cl^- owing to a Cl^--concentration inside the oocyte much smaller than in NFR (Dascal 1987). Figure 3C

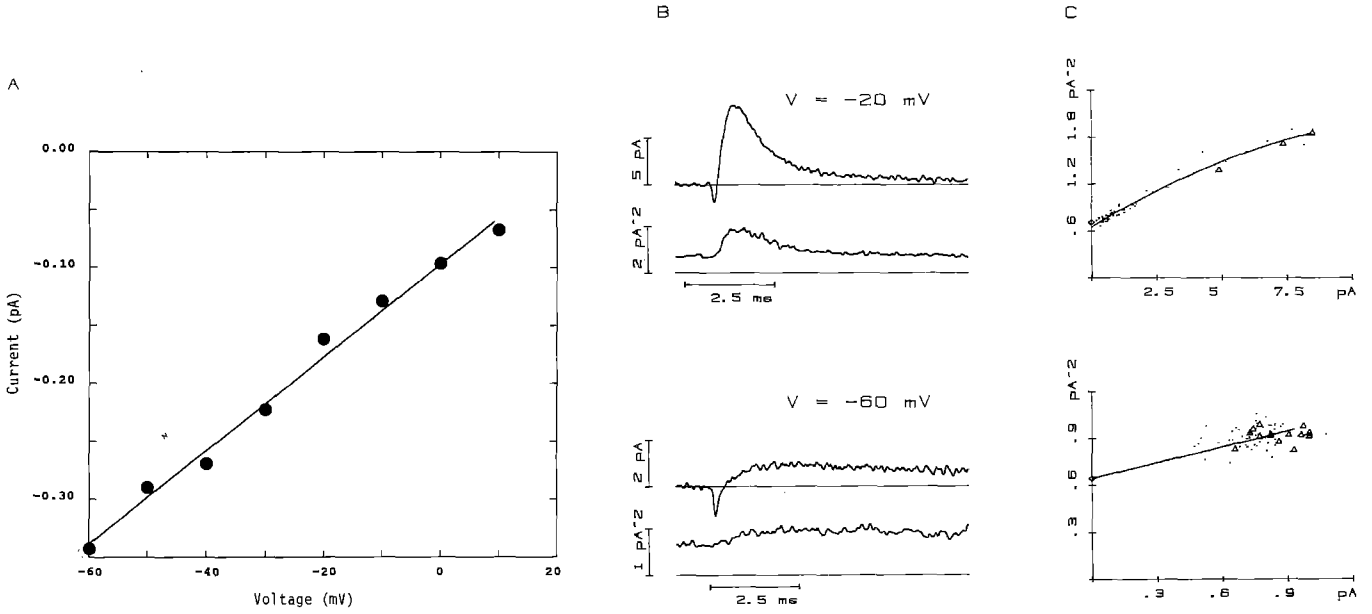

Fig. 2A–C. Noise analysis of mutant E387Q. In **A** a single-channel current-voltage relationship over a large voltage-range is shown. Single-channel currents (filled circles) obtained by noise analysis (see **B** and **C**) from one inside-out patch are plotted versus test voltage. Pipette solution: NFR; bath (internal) solution: 30 m*M* NaCl, 90 m*M* KCl, 10 m*M* HEPES, 10 m*M* EGTA, pH 7.2. The straight line represents a linear regression line ($r=0.99$) with a slope of 4.0 ± 0.2 pS and an extrapolated reversal potential of 24 ± 2 mV. **B** displays typical (inverted) mean current and variance traces at -20 mV (upper traces, 100 averages) and -60 mV (lower traces, 200 averages). Traces were digitally filtered at 4 kHz for display. In **C** are shown the corresponding variance-currents plots. Triangles represent data-points in the rising phase of the current and dots were obtained from the falling phase. The diamond on the variance axis indicates the baseline-variance. Solid lines were obtained by fitting a parabolic function yielding the following parameters: -20 mV: $i=-0.16$ pA, number of channels $=160$; -60 mV: $i=-0.34$ pA (the number of channels was fixed to 200). (For details of the analysis, see Heinemann and Conti 1991)

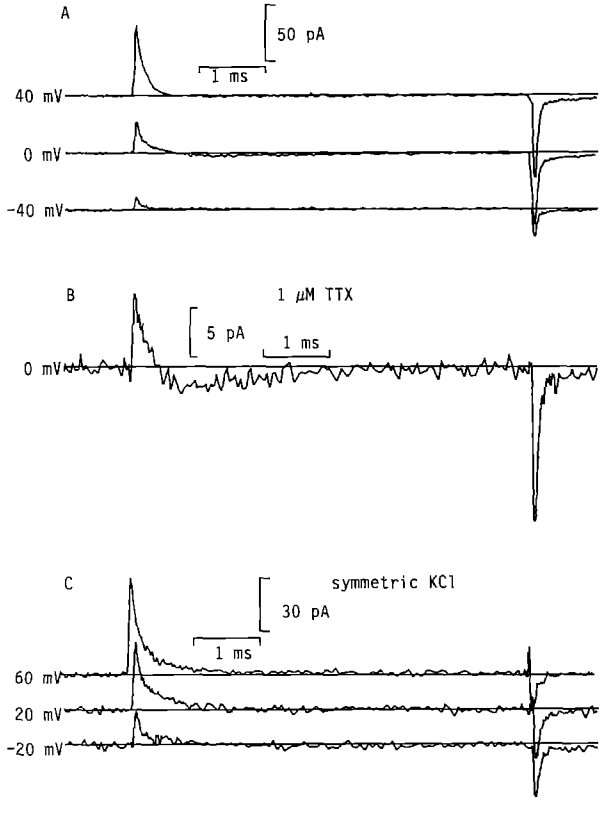

shows that the channel is also practically impermeable to K^+, because only gating currents are detectable from an inside-out patch in symmetrical 100 m*M* KCl solutions. To test qualitatively the permeability of mutant D384N for cations other than Na^+ and K^+ we measured currents in cell-attached patches with pipettes filled with 120 m*M* solutions of LiCl, or NH_4Cl, or CsCl, or RbCl or TMACl, or TEACl, or with 80 m*M* solutions of $CaCl_2$, or $MgCl_2$. In each case, gating currents could be observed, but the relative size of detectable ionic current, if any, as compared to I_g was always smaller than in experiments with NFR. Therefore, we conclude that the ionic pathway gated by mutant D384N is not substantially permeable for any of the cations listed above.

Fig. 3A–C. Voltage-clamp currents of mutant D384N. In **A** are shown traces from a cell-attached patch with NFR in the recording pipette obtained by stepping the membrane voltage from the holding voltage of -100 mV to the indicated values. The intracellular potential of the oocyte was monitored with a microelectode, filled with 2 *M* KCl. The trace in **B** was obtained under identical conditions as the traces in **A** except that 1 μ*M* TTX was included in the pipette filling solution. **C** shows current traces from an inside-out patch from a different oocyte than in **A** (holding voltage in **C**: -97 mV). The solution in **C** was (symmetrical): 10 m*M* HEPES, 10 m*M* EGTA, 100 m*M* KCl, pH 7.2. In **A, B,** and **C** linear leakage and capacitive currents were subtracted by a P/4 method with a "P/4 holding" of -140 mV, pulse length was 6 ms

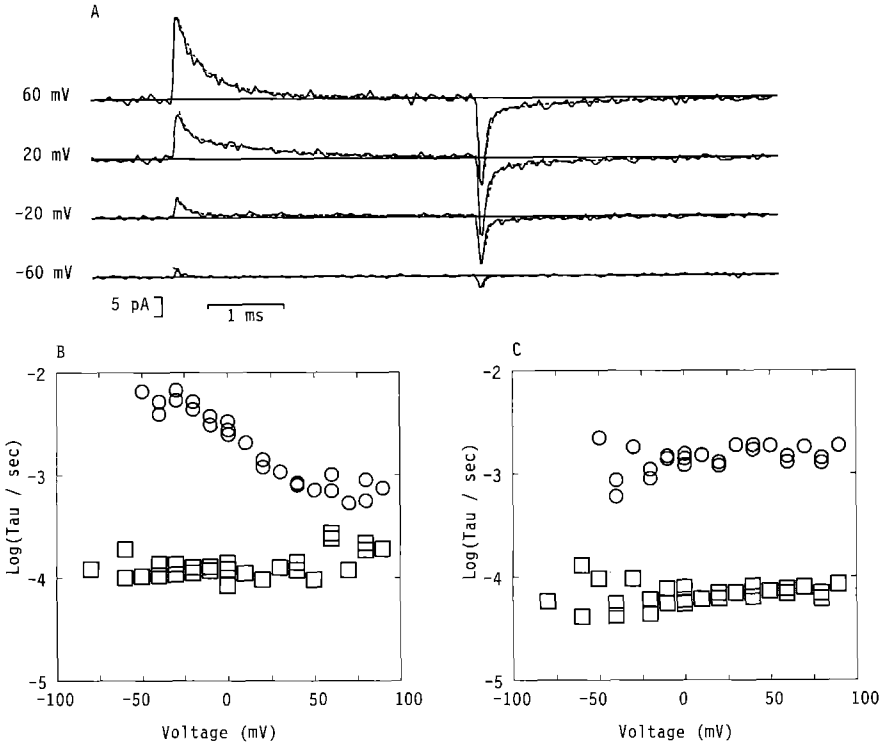

Fig. 4A–C. Gating currents of mutant D384N and kinetic parameters. **A** shows example records of one inside-out patch recorded with the following solutions (in m*M*): Bath: 120 sorbitol, 10 *Tris*Cl, 1.8 EGTA, pH 7.2; pipette: 120 sorbitol, 10 *Tris*Cl, 1.8 $CaCl_2$, pH 7.2. Linear leakage and capacity currents were subtracted as described in *Methods*. Holding voltage was −100 mV. The dashed lines represent fits of (1) to the *On* or *Off* currents. The time-constants obtained by fitting (1) to all current traces of the patch are shown in **B** for the *On* and in **C** for the *Off* response as a function of the test-pulse voltage. τ_{fast} (open squares), and, τ_{slow} (open circles) (see (1)), are plotted on a logarithmic scale

Quantitative analysis of gating current of mutant D384N

The voltage dependence of I_g records shown in Fig. 3A and Fig. 3C is similar to that observed for the wild-type (Conti and Stühmer 1989) except that the gating charge, Q_g, estimated from the time integral of I_g, seems to reach its half saturation value at more positive voltages than normal. However, a trustworthy quantitative analysis of Q_g with solutions of normal ionic strength is prevented by the impossibility of using TTX as a pore-blocker (Fig. 3B). Therefore, to avoid any contamination of I_g by ionic currents, we performed measurements on two inside-out patches with pipette- and bath-solution of very low ionic strength and containing sorbitol as the main osmotic constituent (see legend of Fig. 4).

Figure 4A shows sample records obtained from one such patch. I_g's were elicited by positive voltage pulses superimposed on a holding voltage of −100 mV. The responses shown in the figure were obtained for test pulses to voltages of between −60 and 60 mV increasing in 40 mV steps. After a fast rising phase, both *On* and *Off* currents, decay to negligible values within few milliseconds. For low voltages (< −50 mV), both *On* and *Off* currents could be well fitted with a single exponential. However, for voltages ≥ −50 mV, the sum of two exponential functions was needed to fit the whole time course of the currents. Fits are shown in Fig. 4A as dashed lines. In Fig. 4B and Fig. 4C are plotted the parameters obtained from the fit, respectively to the *On* and to the *Off* phase, of the sum of two exponential functions

$$I(t) = I_{fast} \exp(-t/\tau_{fast}) + I_{slow} \exp(-t/\tau_{slow}) \ . \quad (1)$$

The time constants, τ_{fast} (fast time constant, open squares), and τ_{slow} (slow time constant, open circles), are plotted on logarithmic scale as a function of the pulse voltage.

As expected if the *Off* process is really a double-exponential relaxation, both time constants of the *Off* process do not show any systematic dependence on the test-pulse voltage, and appear to be solely determined by the after-pulse voltage (Fig. 4C). For test-pulses positive to −30 mV, which yielded fairly large I_g's and, therefore, the most accurate estimates of the time constants, the latter had mean values $\tau_{fast} = 70 \pm 20$ μs and $\tau_{slow} = 1.5 \pm 0.3$ ms.

More surprisingly, the fast time constant of the *On* current, in the range of 100 to 150 μs, also depends little on voltage. On the other hand, τ_{slow} for the *On* current decreases from ≈6.5 ms at −50 mV to ≈0.7 ms at voltages ≥40 mV. Because ionic currents are difficult to measure in this mutant, it is difficult to decide whether the various time constants that describe gating current relaxations correspond to the time constants that characterize the open-close kinetics of the low-conductance pore.

The percentage of the contribution of the slow component to the total gating charge was calculated as

$$P_{slow} = 100 \frac{I_{slow}\, \tau_{slow}}{I_{slow}\, \tau_{slow} + I_{fast}\, \tau_{fast}} \quad (2)$$

In the *Off* current P_{slow} rose from negligible values at voltages < −50 mV to a saturating level of ≈50% above $V = -10$ mV. This behavior is consistent with a tentative interpretation of the slow *Off* current as being associated with recovery from a presumably normal inactivation.

In contrast, the voltage-dependence of P_{slow} for the *On* current is broad and bell-shaped with maximal values of ≈80% between −25 and 50 mV. The existence of two distinguishable kinetic components of the *On* current in-

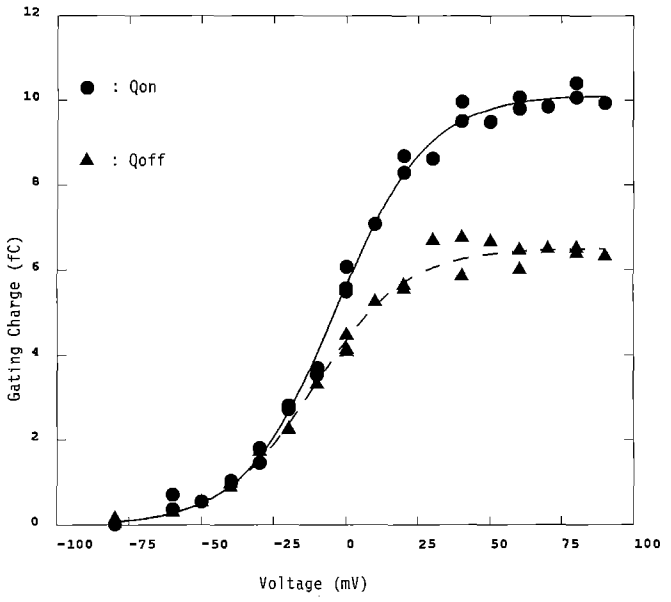

Fig. 5. Charge voltage relationship of mutant D384N. The *On* charge (filled cirlces) and *Off* charge (filled triangles) was obtained by integrating the current traces of one patch (see Fig. 4) over the pulse duration. The solid and dashed line represent fits of (3) to *On* ≥and *Off* charge respectively, with $Q_{max}=10$ fC, $z_q=1.6$ and $V_{1/2}=-3.5$ mV (*On*) and $Q_{max}=6.5$ fC, $z_q=1.6$ and $V_{1/2}=-11$ mV (*Off*)

dicates that the gating of mutant D384N involves at least two different conformational transitions, one of which might be related to inactivation.

The voltage dependence of the *On* and *Off* charge, Q_{on} and Q_{off}, obtained by integrating the currents traces for 4 ms, is shown in Fig. 5 for the same patch as in Fig. 4.

The solid line is a fit to the Q_{on} data of a Boltzmann distribution

$$Q(V)=\frac{Q_{max}}{1+\exp\left(\frac{z_q F(V_{1/2}-V)}{RT}\right)}, \quad (3)$$

where Q_{max} is the maximal charge, z_q is the apparent valence of the gating charge, and $V_{1/2}$ is the mid-point voltage (F=Faraday constant, R=Gas constant, T=Temperature). The nonlinear fit parameters for Q_{on} in Fig. 5 are $V_{1/2}=-3.5$ mV and $z_q=1.6$, whereas for another patch we obtained $V_{1/2}=-14$ mV and $z_q=1.9$. Both estimates of the midpoint voltages are shifted to more positive voltages when compared with the wild-type channel, where $V_{1/2}$ was reported to have a mean value of −23 mV (Conti and Stühmer 1989). The fit of (3) should be considered as purely descriptive, since in general a more complex $Q-V$ dependence is expected in case of the multiexponential kinetics observed for mutant D384N.

Q_{off} is smaller than Q_{on} for voltages >-30 mV, and it reaches a saturating level of about 0.65 Q_{max} at high voltages. This value is larger than reported for natural and exogenous wild-type Na^+ channels where "immobilization" of the gating charge is about 70% (Armstrong and Bezanilla 1977; Conti and Stühmer 1989). However, it should be noted that the integration time that we used for the Q_{off} estimates was much longer than usual, owing to the stability of the baseline. The longer tail duration used in the present data may be the major reason for the clear detection of a slower time constant in the *Off* current. Alternatively, it is possible that this slow component is faster than normal and the consequent larger Q_{off} reflects a faster recovery from inactivation. If we consider as "non-immobilized" only the *Off* charge that is associated with the fast component of the *Off* current, we conclude that only half of the *Off* charge is quickly recovered in the repolarization phase after high test-pulse voltages. With this definition the immobilized gating charge would also attain a saturating value of about 70% in our case.

Discussion

By using non-stationary noise-analysis and gating current measurements we have been able in this work to characterize some important properties of mutant Na^+ channels with "open" states of very low conductance. This shows that these techniques are powerful tools in the investigation of structure-function relationships in voltage-gated channels, allowing an extension of these studies to a wide conceivable variety of in vitro engineered mutants that are non-functional or that have low activity in the normal physiological sense. In particular, our present results show that residues E387 and D384 are essential for the formation of a normal permeation pathway of sodium ions, although their mutation does not produce any marked change in the gating of the Na^+ channel.

The single-channel conductance of the TTX-insensitive mutant E387Q was estimated to be ≈5 times smaller than that of the wild-type TTX-sensitive channel. Although still highly selective for Na^+ over K^+ the open pore of mutant E387Q has a linear *i*-V characteristic over a wide voltage range even under asymmetric ionic conditions, in marked contrast with the wild-type behavior. The properties of mutant E387Q resemble closely those of natural channels exposed to trimethyloxonium (TMO). TMO treatment of frog Na^+ channels yields a three-fold reduction of γ with little modification of gating, a loss of TTX sensitivity, and a more linear instantaneous I-V (Spalding 1980; Sigworth and Spalding 1980). It is possible that TMO acts by methylation of residue E387 and/or other acidic side chains located in proximity to the extracellular mouth of the pore.

We have been able to show that mutant D384N is expressed and inserted in the membrane of *Xenopus* oocytes although its "open" state has an extremely low conductance. Expression was detected by measuring the gating currents, I_g, associated with the voltage-dependent conformational transitions of the mutant channel. The I_g and Q-V properties of D384N are rather similar to the wild-type, suggesting that neutralizing aspartic acid D384 has modified only the conductivity of the pore, but not the mechanism that is normally associated with the gating. The fact that the gating currents of mutant D384N, observed in the absence of TTX, are similar to those obtained for the wild-type in the presence of TTX (Conti and Stühmer 1989), supports indirectly the common assumption that TTX binding does not affect I_g.

The two mutations investigated in this study are confined to a limited region in the large Na^+ channel protein whose alteration greatly influences the conductance properties and toxin sensitivity. It is tempting to suggest that this region participates in forming the extracellular mouth and/or the lining of the pore itself (Guy and Conti 1990). However, this conclusion can only be validated by further investigations of other mutations in the same region and in equivalent regions of the other three repeats of the Na^+ channel.

Acknowledgements. We thank Drs. K. Imoto and T. Lamb for comments on the manuscript. MP was supported by EEC grant No. SC1*305. This investigation was also partially supported by the EEC grant No. SC1*CT90-0463, by Japanese research grants from the Ministry of Education, Science and Culture, the Science and Technology Agency, the Mitsubishi Foundation and the Foundation of Metabolism and Diseases, and the Italian Progetto Finalizzato Ingeneria Genetic del CNR.

References

Almers W (1978) Gating currents and charge movements in excitable membranes. Rev Physiol Biochem Pharmacol 82:96–190

Armstrong M, Bezanilla F (1973) Currents related to the gating particles of sodium channels. Nature (London) 242:459–461

Armstrong M, Bezanilla F (1977) Inactivation of the sodium channel. II. Gating current experiments. J Gen Physiol 70:567–590

Bezanilla F, Armstrong M (1977) Inactivation of the sodium channel. J Gen Physiol 70:549–566

Conti F, Stühmer W (1989) Quantal charge redistributions accompanying the structual transitions of sodium channels. Eur Biophys J 17:53–59

Conti F, Neumcke B, Nonner W, Stämpfli R (1980) Conductance fluctuations from the inactivation process of sodium channels in myelinated nerve fibres. J Physiol (London) 308:217–239

Conti F, Inoue I, Stühmer W (1984) Pressure dependence of sodium gating currents in the squid giant axon. Eur Biophys J 11:137–147

Dascal N (1987) The use of *Xenopus* oocytes for the study of ion channels. CRC Crit Rev Biochem 22:317–387

Guy HR, Conti F (1990) Pursuing the structure and function of voltage-gated channels. Trends Neurosi 13:201 – 206

Hamill OP, Marty A, Neher E, Sakmann B, Sigworth FJ (1981) Improved patch-clamp techniques for high-resolution current recording from cells and cell-free membrane patches. Pflügers Arch 391:85–100

Heinemann SH, Conti F (1991) Non-stationary noise analysis and its application to patch clamp recordings. In: Rudy B, Iverson LE (eds) Methods in enzymology (In press)

Hille B (1984) Ionic channels of excitable membranes. Sinauer Sunderland, Mass

Methfessel C, Witzemann V, Takahashi T, Mishina M, Numa S, Sakmann B (1987) Patch clamp measurements on *Xenopus* laevis oocytes: currents through endogeneous channels and implanted acetylcholine receptor and sodium channels. Pflügers Arch 407:577–588

Noda M, Ikeda T, Kayano T, Suzuki H, Takeshima H, Kurasaki M, Takahashi H, Numa S (1986a) Existence of distinct sodium channel messenger RNAs in rat brain. Nature (London) 320:188–192

Noda M, Ikeda T, Suzuki H, Takeshima H, Takahashi T, Kuno M, Numa S (1986b) Expression of functional sodium channels from cloned cDNA. Nature (London) 322:826–828

Noda M, Suzuki H, Numa S, Stühmer W (1989) A single point mutation confers tetrodotoxin and saxitoxin insensitivity on the sodium channel II. FEBS Lett 259:213–216

Pusch M (1990a) Open-channel block of Na^+ channels by intracellular Mg^{2+}. Eur Biophys J 18:317–326

Pusch M (1990b) Divalent cations as probes for structure-function relationships of cloned voltage-dependent sodium channels. Eur Biophys J 18:327–333

Pusch M, Conti F, Stühmer W (1989) Intracellular magnesium blocks sodium outward currents in a voltage- and dose-dependent manner. Biophys J 55:1267–1271

Pusch M, Noda M, Conti F (1991) Gating currents of a sodium-channel mutant with very low conductance. (abstr). Biophys J 59:25a

Sigworth FJ (1977) Sodium channels in nerve apparently have two conductance states. Nature (London) 270:265–267

Sigworth FJ, Spalding BC (1980) Chemical modification reduce the conductance of sodium channels in nerve. Nature (London) 283:293–295

Spalding BC (1980) Properties of toxin-resistant sodium channels produced by chemical modification in frog skeletal muscle. J Physiol (London) 305:485–500

Stühmer W, Methfessel C, Sakmann B, Noda M, Numa S (1987) Patch clamp characterization of sodium channels expressed from rat brain cDNA. Eur Biophys J 14:131–138

Stühmer W, Conti F, Suzuki H, Wang X, Noda M, Yahagi N, Kubo H, Numa S (1989) Structural parts involved in activation and inactivation of the sodium channel. Nature (London) 339:597–603

Tejedor FJ, Catterall WA (1988) Site of covalent attachment of α-scorpion toxin derivatives in domain I of the sodium channel subunit. Proc Natl Acad Sci USA 85:8742–8746